On the Evolution of Thunderstorm Rotation

RICHARD ROTUNNO

National Center for Atmospheric Research,[1] Boulder, CO 80307

(Manuscript received 24 August 1980, in final form 21 November 1980)

ABSTRACT

A vertical velocity field is chosen which imitates that of the initial stages of cloud development as simulated numerically by Wilhelmson and Klemp (1978). Given this, an approximate version of the equation for the vertical component of the vorticity is solved. The vertical velocity is assumed to vary with height as $\sin \pi z/H$, where z is the altitude and H is the depth of the domain. At the level of nondivergence ($z = H/2$), the solutions indicate the development of a vortex pair which then splits into two vortex pairs one moving to the right of the mean wind and the other to the left (as observed in the numerical model). At lower levels, owing to the convergence in the updraft and divergence in the downdraft, the cyclonic/anticyclonic member of the vortex pair in the rightward/leftward moving storm is greatly enhanced. The vorticity maximum is initially on the maximum gradient of vertical velocity. At mid-levels the maximum vorticity migrates with time close to the position of maximum vertical velocity. However, at lower levels, the maximum vorticity migrates with time past the position of maximum vertical velocity and thereafter resides on the vertical velocity gradient separating updraft from downdraft, as observed in a number of case studies. Some general comparisons of the present theory with an observational case study are made.

1. Introduction

The past few years have witnessed the development of three-dimensional numerical models of severe thunderstorms (see, e.g., Lilly, 1979). These models are solutions to the Navier-Stokes equations with important buoyancy effects owing mainly to phase changes of water. While these models have many limitations (Clark, 1979), it appears they can do remarkably well in simulating at least some aspects of severe storms. For example, severe storms (or more precisely their associated radar echoes) travel somewhat slower than and to the right of the mean wind (Huff *et al.*, 1954). This feature appears strikingly in the simulations of Wilhelmson and Klemp (1978, hereafter referred to as WK) as a rain pattern[2] which moves to the right of the mean wind. Other features common to almost all severe storms (e.g., the gust front, the hook echo, the anvil and others[3]) are easily identified in model simulations (Klemp *et al.*, 1979). The appearance of these features is, at least, circumstantial evidence the numerical model contains the relevant physical processes.

One such feature of immense importance to the theory and actuality of tornadoes is the *mesocyclone*. The mesocyclone is a rotating cumulonimbus cell [a tornado cyclone is a mesocyclone which contains a tornado (Davies-Jones, 1980)] and it is with the evolution of this rotation that this report is concerned. To say that storm rotation is related to the pattern of updraft and downdraft within the storm is a gross understatement in view of numerical modeling studies. For example, Schlesinger (1975), in his case P2 takes as a basic state a westerly flow which increases with height and a potentially unstable distribution (again only with height) of temperature and water vapor. Initially, vortex lines are horizontal (i.e., they point toward the north by the right-hand rule). Vertical motion is initiated by an isolated warm spot; the vortex lines move with the fluid[4] hence do not remain horizontal, i.e., a vertical component is developed where there was *none* initially. This process is graphically described as vortex line tilting (see, e.g., Dutton, 1976, p. 341). The hypothesis that this mechanism is a major contributor to storm rotation was advanced by Barnes (1970). Barnes' conceptual picture (see his Fig. 16) consists of a rotating storm cell traveling at an angle with respect to a mean wind which increases with height. The typical situation has a westerly mean wind with

[1] The National Center for Atmospheric Research is sponsored by the National Science Foundation.

[2] Since rain and hail are the cause of the radar echo, movement of the model-generated rain pattern is associated with movement of the radar echo.

[3] These terms are part of the lexicon of severe storm research; definitions are given, where appropriate, within the text.

[4] This is strictly true only for an inviscid, barotropic fluid.

0027-0644/81/030577-10$06.50

the storm moving, as noted above, somewhat slower than and to the right (facing east) of the mean wind. Given this scenario, it was demonstrated by Barnes that this rightward moving storm tilts the horizontal vortex lines of the wind shear into the positive vertical direction and a cyclonically rotating storm is sustained.

Although both Barnes (1970) and Schlesinger (1975) invoke vortex line tilting as an explanation for the rotating storm, there is little resemblance between Schlesinger's numerical model solution (which produces a vortex doublet) and Barnes single-signed traveling vortex. It is important to note Schlesinger's integrations were over a relatively short time period (~12.5 min). When longer integrations were achieved (see Schlesinger, 1978; WK), the resulting flow fields were, at low levels, in accord with the concept of a cyclonically rotating storm traveling to the right of the mean wind.[5]

The present work is limited in scope, that is, no comprehensive theory of storm movement is profferred. The principal concern is, as already mentioned, the evolution of storm rotation. I have found that it is possible to describe the evolution of the storm's rotation as it occurs in the numerical models by a simple analytical model. In the early stages of cumulus development it is assumed the vertical velocity distribution is mainly determined by the buoyancy distribution (latent heating; rain formation and descent which introduce effective negative buoyancy through loading; also evaporative cooling). The details of the buoyancy distribution are hopelessly complicated from an analytical perspective, depending as they do on the presence of condensation nuclei, accretion rates, etc. Thus, I ask a limited question: What is the consequent field of the vertical vorticity $\zeta(x, y, z, t)$, given a field of vertical velocity $w(x, y, z, t)$ in a flow with mean horizontal velocity components $\bar{U}(z)$? There is nothing particularly novel in this approach. Indeed, it was Ferrel (1889) who hypothesized that tornadoes form when an updraft meets with a "gyratory" wind field, the updraft presumably being caused by buoyancy effects. That is, Ferrel's problem can be posed in the same way, given an updraft, the vertical vorticity equation (neglecting tilting) can be solved to obtain amplification of vorticity by convergence of an initial vorticity (gyratory wind) field. The vortex-tilting argument of Barnes (1970) may be viewed as a similar vein. What is novel in the present work in the somewhat more rigorous development of this approach by specifying a $w = w(x, y, z, t)$ which closely resembles those in a numerical model study (WK) and (possibly) in nature (Bluestein and Sohl, 1979) and then solving an approximate version of the equation for the vertical vorticity.

In the discussion to follow, reference to mid-level is synonymous with the level of zero divergence, while reference to the low-level means that convergence (divergence) is nonzero. Flow above mid-levels is not addressed in this paper.

The results may be summarized as follows:

1) During the initial stage a symmetric isolated updraft is prescribed, in westerly wind which increases with height. A vortex pair (cyclonic on the right, anticyclonic on the left) is produced by the analytical model. Lower and mid-level solutions are similar.

2) The next phase begins with a weakening of the vertical velocity in the center of the updraft prescribed. The vertical vorticity solution then gives two vortex pairs on either side of the original line of symmetry. Owing to vortex stretching, the lower level vorticity extrema are larger than those of the mid-level.

3) The final point to which this calculation is carried is where the central updraft has weakened to the point of becoming a downdraft with a surrounding updraft. I then prescribe that these updraft/downdraft pairs move to the right and left of the mean wind with velocities $\mp \alpha$, respectively. The response is that each vortex pair follows the prescribed movement of the updraft/downdraft pair. In the mid-level the magnitude of the positive/negative part of the vortex is slightly less than the magnitude of the negative/positive part for the rightward/leftward moving pair. At low levels, as observed in WK, the rightward/leftward moving storm is dominated by positive/negative vorticity.

The reason for this is that owing to the nonzero convergence, the vorticity on the updraft side is stretched and intensified while the vorticity on the downdraft side is compressed and diminished leaving a cyclonic/anticyclonic vortex travelling to the right/left of the mean wind.

2. The vorticity equation

Sufficient for the present study is the set of equations developed by Ogura and Phillips (1962) called the shallow anelastic, Boussinesq equations; i.e.,

$$\frac{\partial \mathbf{v}}{\partial t} + \mathbf{v}\cdot\nabla\mathbf{v} = -c_p\theta_0\nabla\pi + B\mathbf{k}, \tag{1}$$

$$\nabla\cdot\mathbf{v} = 0, \tag{2}$$

where $\mathbf{v}$ is the velocity vector, θ_0 a reference potential temperature, c_p the specific heat of air at constant pressure, $\mathbf{k}$ is the unit vector in the vertical direction, and

$$\pi \equiv \left(\frac{P}{P_0}\right)^{R/c_p}, \tag{3}$$

[5] But also contain a mirror image anticyclonically rotating storm travelling to the left of the mean wind. This problem is briefly addressed in Section 6.

where P, P_0 and R are the pressure, ground pressure and gas constant, respectively. An equation for B, which represents the cumulative effect of all contributions to buoyancy (latent heating, raindrop drag, etc.) is not included because it will not be used. As a point of reference, recall that $B = g\theta/\theta_0$ for a dry atmosphere.

Upon taking the curl of (1) and using (2) we obtain

$$\frac{\partial \boldsymbol{\omega}}{\partial t} = -\mathbf{v}\cdot\nabla\boldsymbol{\omega} + \boldsymbol{\omega}\cdot\nabla\mathbf{v} + \nabla \times B\mathbf{k}, \qquad (4)$$

$$\text{A} \qquad \text{B} \qquad \text{C}$$

where $\boldsymbol{\omega}$ = curl v is the vorticity vector. In words, Eq. (4) expresses that the vorticity at a location can be changed by (A) advection of vorticity, (B) changes in the orientation and length of vortex-tubes (see Batchelor, 1967, p. 268) and (C) baroclinicity, i.e., the extent to which level surfaces of density and pressure are non-parallel. To achieve the stated purpose—a quantitative study of the evolution of storm rotation—consider the vertical component of (4), i.e.,

$$\frac{\partial \zeta}{\partial t} = -\mathbf{v}\cdot\nabla\zeta + \boldsymbol{\omega}\cdot\nabla w. \qquad (5)$$

That the baroclinic terms do not appear in this equation is a consequence of the Boussinesq approximation.

The second term on the right-hand side is often written as

$$\boldsymbol{\omega}\cdot\nabla w = \mathbf{k}\cdot\left(\frac{\partial \mathbf{v}_H}{\partial z} \times \nabla_H w\right) + \zeta\frac{\partial w}{\partial z}, \qquad (6)$$

where the first and second terms on the right-hand side are the tilting and stretching terms, respectively; the subscript H denotes the horizontal component of a vector. The following definitions save some writing below:

$$T \equiv \mathbf{k}\cdot\left(\frac{\partial \mathbf{v}_H}{\partial z} \times \nabla_H w\right), \quad S = \frac{\partial w}{\partial z}. \qquad (7a, b)$$

Thus (5) can be written as

$$\frac{d\zeta}{dt} - S\zeta = T, \qquad (8)$$

which can be interpreted as the equation governing the rate of change of the vertical component of the vorticity vector following a piece of fluid as it moves. In this Lagrangian description the integral of (8) is

$$\zeta(t) = \exp\left[\int^t S(t')dt'\right] \times \left\{\int^t T(t')\exp\left[-\int^{t'} S(t'')dt''\right]dt' + \zeta(0)\right\}. \qquad (9)$$

Of course, this relationship is purely formal since one needs to know the path a fluid parcel will take *a priori* to evaluate the integrals in (9). This knowledge, necessarily, is lacking since changes in a parcel's vorticity relative to surrounding parcels will surely alter its path of travel and the values of T and S. However, an examination of the structure of (9) is illuminating and germane to the results which follow. If $T = 0$, Eq. (9) states that the parcel's initial vorticity shall increase or decrease, according to the amount of time it spends in places where S is positive (convergence) or negative (divergence). The simple case where S = constant indicates exponential amplification/decay for $S \gtrless 0$. For $T \neq 0$, a parcel which possesses rotation about a horizontal axis is tilted so that it has a component of rotation about a vertical axis. This vertical vorticity, so produced, can then be stretched/compressed as described above.

I return for the remainder of this paper to the Eulerian equation (5). To proceed toward a solution, some approximations must be made; these are discussed in Section 3.

3. An approximate vorticity equation

a. Development

Suppose (1) can be linearized about a mean flow in the x-direction $\bar{U}(z)$. The vorticity equation (5) becomes

$$\frac{\partial \zeta}{\partial t} + \bar{U}(z)\frac{\partial \zeta}{\partial x} = \frac{\partial \bar{U}}{\partial z}\frac{\partial w}{\partial y}. \qquad (10)$$

Thus, (10) contains a linearized version of the advection and tilting terms, however, because $\bar{U}$ is a function of z only and the earth's rotation has been neglected, there is no stretching term. But we know from observations by Ray (1976), Bluestein and Sohl (1979) and Brandes (1978) that stretching is important. Hence I add the stretching term to (10) to obtain

$$\frac{\partial \zeta}{\partial t} + U_s\frac{\partial \zeta}{\partial x} = \frac{\partial \bar{U}}{\partial z}\frac{\partial w}{\partial y} + \zeta\frac{\partial w}{\partial z}. \qquad (11)$$

The addition of this term must be regarded as purely *ad hoc* since I shall continue to neglect the nonlinear advection and nonlinear tilting terms. This is difficult to justify rigorously. However, let me offer the following heuristic arguments. The question of how a storm acquires rotation about a vertical axis can be answered by examining how the vertical component of the vorticity vector (ζ) develops as a function of space and time. One suspects large values of ζ to be indicative of strong rotation. The discussion of Eq. (9) showed that the tilting term acts as a source of ζ and that stretching can act to exponentially amplify the source. Now, the effect of advection can only increase ζ up to the

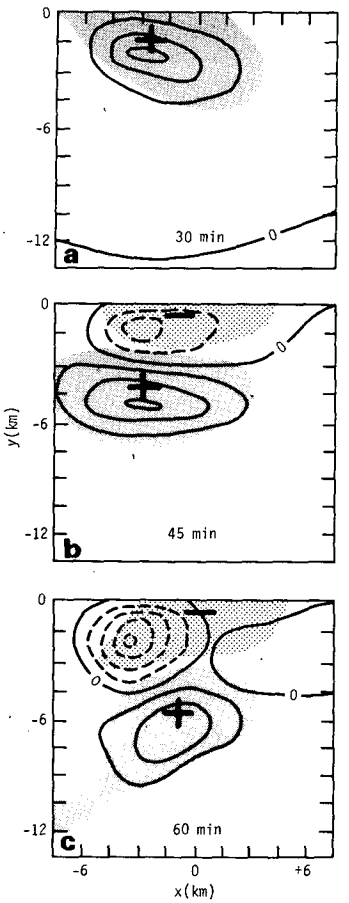

FIG. 1. Results of the numerical storm model of Wilhelmson and Klemp (1978). Horizontal cross sections of vertical vorticity at 1.75 km at (a) 30 min, (b) 45 min and (c) 60 min. The contour interval is 2×10^{-3} s^{-1}. Solid lines indicate positive values and dashed lines negative values. In the light shaded area $w < -1$ m s^{-1} and in the dark area $w > 1$ m s^{-1}, and minus signs, respectively. Maximum updrafts and downdrafts are indicated by plus and minus signs, respectively. (After Wilhelmson and Klemp, 1978).

maximum value already existing in the domain. So, in a theory of how storm rotation (or ζ) becomes large starting from a state of zero rotation, it seems essential that stretching which is a nonlinear term, be included while the other nonlinear terms are neglected in the interest of simplicity. Some support for these assumptions is contained in the analysis of Blechman (1980) where the terms of Eq. (5) for a fine-resolution version of Schlesinger's (1978) model P3 are examined. Fig. 18 of his analysis reveals that the vertical (other components are much smaller) advection is small compared to the stretching term at low to mid-levels (the present analysis is confined to this region), but becomes important from mid to high levels within a developing rotating storm. However, the main justification of Eq. (11) is *a posteriori*, i.e., the solutions are compared to observational data and the more comprehensive model solutions of WK. Since these severe storms are, more or less, erect and travel in the x-direction at some height-averaged speed, I have let $\bar{U} \approx \bar{U}_s$, a constant in the advection terms. Now if somehow we were given $w = w(x, y, z, t)$ associated with a developing cumulonimbus, Eq. (11) then describes the associated development of storm rotation.

If one asks not for a complete theory of storm movement and development, but, for a theory of storm rotation evolution *given* a vertical velocity field which contains the salient features of a developing storm, then one might expect (11) to provide an answer to this admittedly limited question.

So, the procedure of prescribing w to obtain ζ in (11) will be correct to the extent that 1) the approximate equation (11) is valid, and 2) w is independent ζ.[6]

In WK, convection is initiated by a warm symmetric bubble, which produces rising motion sufficient to send air parcels to their LCL; latent heat is released and the strength of the updraft increases with time while remaining symmetric. After a time, the condensed water vapor accumulates into raindrops mostly on the center of the initial updraft; this loads the updraft and weakens it at the center until the original updraft center is now occupied by downdraft. So, the original updraft is divided into *two* updraft/downdraft pairs which move apart from each other; one moves to the right of the mean wind, the other to the left. (An effect of shear is implicitly included here, since in a non-sheared environment the updraft is divided symmetrically, i.e., the downdraft spreads radially outward from the center of the original updraft. The arguments presented below work equally well for this case.) Fig. 1 is reproduced from WK (their Fig. 14) and displays the right-moving development (the left-moving storm is a mirror image and is not shown).

In an attempt to imitate this behavior, I let

$$w' = \frac{2t' \sin\gamma' z'}{(x' - \bar{U}_s' t')^2 + 1} \frac{y'^2 - \alpha t'^2 + 1}{(y'^2 - \alpha t'^2 + 1)^2 + 1}, \quad (12)$$

where

$$(w', \bar{U}') = \frac{1}{w_0}(w, \bar{U}); \quad x', y', z' = \frac{1}{R}(x, y, z);$$

$$\gamma' = \frac{\pi}{H} R; \quad t' = \frac{w_0}{R} t, \quad (13)$$

with w_0, R and H being characteristic vertical velocity, horizontal length and vertical length scales, respectively; α is defined below. Figs. 2a–2c contains a graph of w' vs $-y'$ for $\alpha = 1$, $t' = 0.1$, 1.0

[6] I should emphasize that this approximation will be valid only during the initial stages of storm development; a strong coupling between w and ζ is likely essential to the storm propagation mechanism (K. Emanuel, private communication).

and 2.0, $x' = \bar{U}_s' t'$ and $z' = \pi/2\gamma'$. For $x' \neq \bar{U}_s' t'$, the curve of w' vs $-y'$ has exactly the same shape but diminished amplitude. Letting $\zeta' = (R/w_0)\zeta$, Eq. (11) becomes

$$\frac{\partial \zeta'}{\partial t'} + \bar{U}_s' \frac{\partial \zeta'}{\partial x'} = \frac{\partial \bar{U}'}{\partial z'} \frac{\partial w'}{\partial y'} + \zeta' \frac{\partial w'}{\partial z'} . \quad (14)$$

The variables y' and z' enter (14) as parameters as there are no derivatives of ζ' with respect to y' or z'. To further facilitate the discussion the coordinate axis in the x direction is transformed according to

$$\hat{x} = x' - \bar{U}_s' t'. \quad (15)$$

Eq. (14) is then

$$\frac{\partial \zeta'}{\partial t'} = \frac{\partial \bar{U}'}{\partial z'} \frac{\partial w'}{\partial y} + \zeta' \frac{\partial w'}{\partial z'} . \quad (16)$$

The solution to (16) is

$$\zeta' = \exp\left(\int^{t'} \frac{\partial w'}{\partial z'} d\tilde{t}' \right) \left[\frac{\partial \bar{U}'}{\partial z'} \int_0^{t'} \frac{\partial w'}{\partial y'} \times \exp\left(- \int^{\tilde{t}'} \frac{\partial w}{\partial z} d\tilde{\tilde{t}}' \right) d\tilde{t}' + \zeta'(0) \right] , \quad (17)$$

which bears a strong resemblance to the exact solution in the Lagrangian framework [cf. Eq. (9)].

Substituting (12) into (17) and performing the integration, then yields

$$\zeta' = \frac{\partial \bar{U}'}{\partial z'} \frac{1}{(\xi'^2 + 1)^{\mu}} \frac{2y' \sin\gamma' z'}{\alpha(\hat{x}^2 + 1)} \times \int_{y'^2+1}^{\xi'} (\tilde{\xi}^2 - 1)(\tilde{\xi}^2 + 1)^{\mu-2} d\tilde{\xi}, \quad (18)$$

where

$$\mu \equiv \frac{\gamma' \cos\gamma' z}{2\alpha(\hat{x}^2 + 1)} \quad \text{and} \quad \xi' = y'^2 - \alpha t'^2 + 1.$$

According to Gradshteyn and Ryzhik (1965, p. 71), to evaluate the integral in (18) in terms of elementary functions, μ must be an integer. In what follows consider two cases: $\mu = 0$, which corresponds to the level of nondivergence and $\mu = 1$ which for $\alpha = 1$, $\hat{x} = 0$ corresponds to a level approximately half way between $z' = 0$ and $z' = \pi/2\gamma'$.

b. Solutions $\mu = 0$ (mid-level)

For $\mu = 0$, Eq. (18) becomes

$$\zeta' = -\frac{2y'}{\alpha(\hat{x}^2 + 1)} \frac{\partial \bar{U}'}{\partial z'} \left[\frac{y'^2 - \alpha t'^2 + 1}{(y'^2 - \alpha t'^2 + 1)^2 + 1} - \frac{y'^2 + 1}{(y'^2 + 1)^2 + 1} \right] . \quad (19)$$

Note that while w' is symmetric in y', ζ' is antisymmetric. Fig. 2 depicts w', $\zeta'/(2\partial\bar{U}'/\partial z')$ (dashed curve) vs $-y'$ (with $\alpha = 1$, $\hat{x} = 0$) for $t' = 0.1$, 1.0, 2.0. At $t = 0$ (not shown), $w' = \zeta' = 0$. In the early stage ($t' = 0.1$), w' is positive with a maximum near $y' = 0$. ζ' has positive maximum near the maximum gradient of w'; there also is negative minimum of ζ' on the northern side (not shown). So, there is a

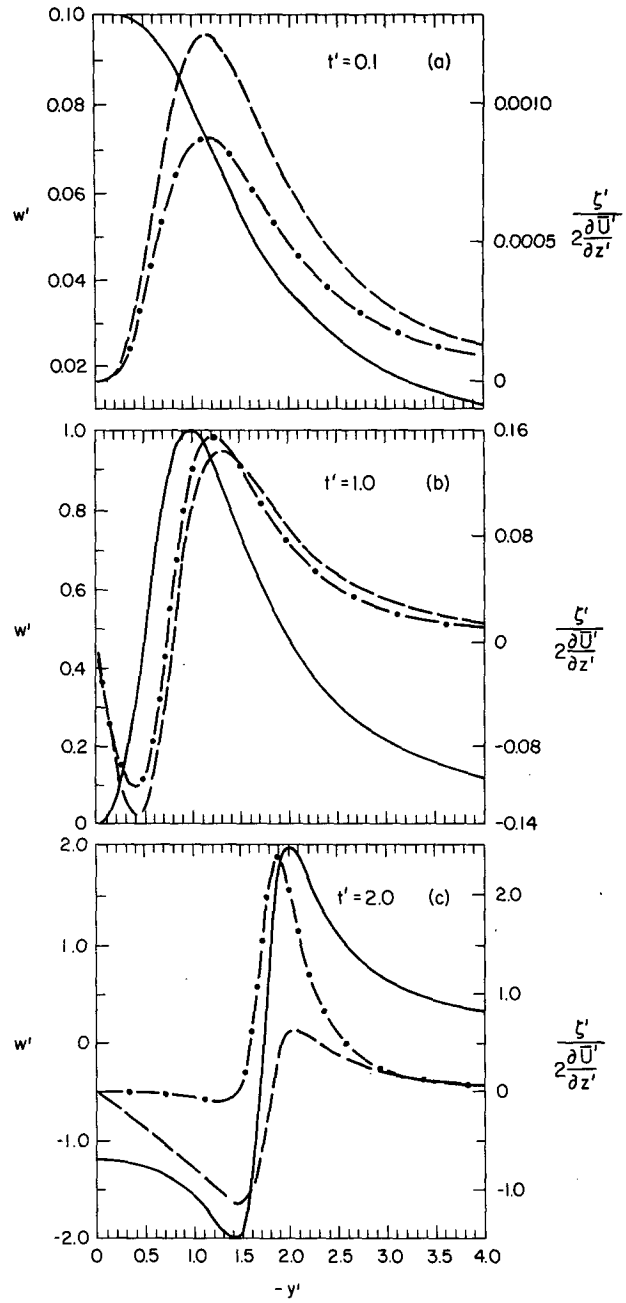

FIG. 2. Nondimensional vertical velocity w' (solid) and vertical vorticity $\zeta'/(2\partial\bar{U}'/\partial z')$ vs $-y'$ for $x' = \bar{U}_s' t'$, (a) $t' = 0.1$, (b) $t' = 1.0$ and (c) $t' = 2.0$ calculated from (12). With w' specified as in (a)–(c), (14) is solved for ζ'. The dashed line corresponds to ζ' at the level where $\partial w'/\partial z' = 0$ [Eq. (19)] and the dash-dotted line corresponds to ζ' at a lower level [Eq. (20)].

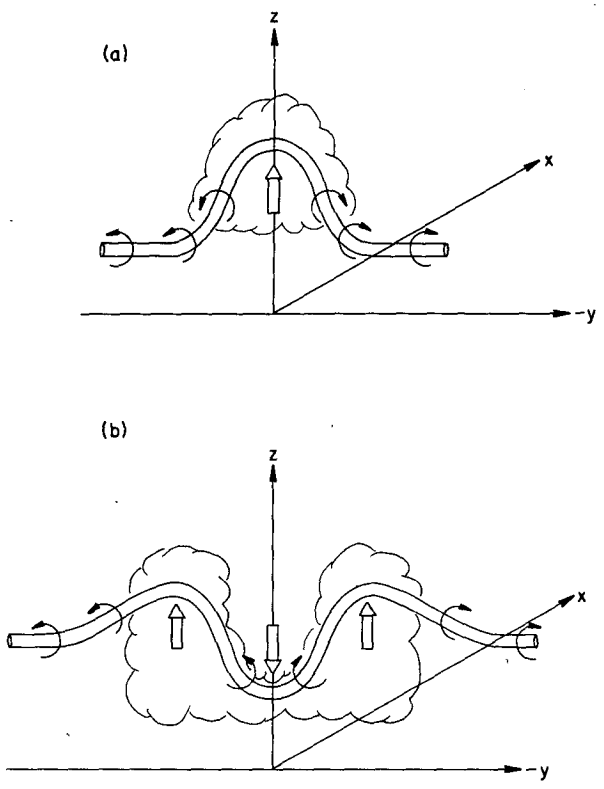

FIG. 3. A schematic of how a typical vortex-tube (associated with the mean wind shear) changes its orientation by interaction with a convective element (a) in the initial stage, the vertical velocity is concentrated, upward and symmetric, so producing cyclonic vorticity on the right (facing east) and anticyclonic on the left. (b) At a later stage, rain forms where the updraft was most intense, loads the updraft and causes the original cell to split. So, we now have two vortex pairs on either side of the x axis. These two stages correspond to the stages shown in Fig. 1 from WK and the dashed line (mid-level) in Figs. 2a and 2b.

vortex pair (cyclonic on the right, anticyclonic on the left). This behavior may be interpreted as the upward tilting of the vortex tubes associated with the mean wind shear (Fig. 3a). An alternate view sometimes expressed in the literature is that the counterrotating vortices are due to an effective obstacle formed by fluid of less horizontal momentum being transported upward, partially (at least) conserving that momentum and so, at the higher level there is, relative to the surrounding flow, a deficit of horizontal momentum (see, e.g., Fulks, 1962). Of course, these phenomena essentially are the same.

The initial updraft continues to grow at $t' = 1.0$, but weakens in the center; ζ' also continues to grow, but now has a negative component near $y' = 0$. The negative vorticity develops in response to the change in sign of $\partial w'/\partial y'$ (Bluestein and Sohl, 1979) as the initial updraft weakens near $y' = 0$. This behavior may again be interpreted in terms of vortex line tilting (Fig. 3b). At the last stage to which this analysis is carried ($t' = 2.0$), the central region of the original updraft is now occupied by downdraft, the vorticity shows slightly more negative vorticity in the downdraft than the positive in the updraft, the ζ' maximum is almost coincident with the w' maximum. Overall there is good agreement between these points and the results of the numerical study of WK shown in Fig. 1.

It is important to note that the vorticity field of Fig. 1 is at $z = 1.75$ km in a domain of a total depth of 10 km; the storm top is ~8 km thus Fig. 1 may be considered a representation of mid-level flow. At $t = 60$ min at $z = 1.75$ m there is still a vortex pair, with slightly larger negative than positive vorticity. This is hard to rectify with Barnes' model of a single-signed traveling vortex. However looking to WK's Fig. 15 (reproduced as Fig. 4) it is evident that *the positive vorticity is strong and completely dominates the negative vorticity at $z = 0.75$ km*. Therefore, there is something about the lower levels that favors the positive sign (in the southern half-plane). As already mentioned, Ray (1976), WK, Bluestein and Sohl (1979), Heymsfield (1978), and Brandes (1978) find that the term in the vertical vorticity equation which corresponds to vortex stretching is important if not dominant, at low levels.

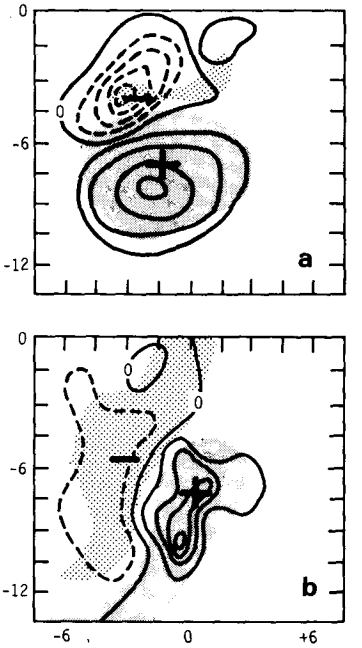

FIG. 4. Horizontal cross sections of vertical vorticity for R20 at 75 min at (a) 2.75 km and (b) 0.75 km. The vorticity is shown with a contour interval of 2×10^{-3} s^{-1}. Solid lines indicate positive values and dashed lines negative values. In the light-shaded area $w < -1$ m s^{-1} and in the dark area $w > 1$ m s^{-1}. Maximum updraft and downdraft locations are indicated by plus and minus signs, respectively. (After Wilhelmson and Klemp, 1978).

c. Solutions at a lower level ($\mu = 1$)

Letting $\mu = 1$ with $\alpha = 1$ and $\hat{x} = 0$ yields $z' = \gamma'^{-1} \cos^{-1}(2/\gamma')$. Recall $\gamma' = \pi R/H$; if $R \sim H$ then $\gamma' \sim \pi$. Thus at $z' = 0.253$, Eq. (18) becomes

$$\frac{\zeta'}{2\partial \bar{U}'/\partial z'} = -y' \sin(0.253\pi)(1 + \xi')^{-1} \times (2 \tan^{-1}\xi' - 2 \tan^{-1}\xi'_{t=0} - \xi' + \xi'_{t=0}). \quad (20)$$

Figs. 2a–2c display Eq. (20). Again at $t' = 0$, $\zeta' = 0$ (not shown). At $t' = 0.1$ the solutions are almost the same as those with $\mu = 0$. At $t' = 1.0$, the vorticity extrema are somewhat larger in the stretched case; this is to be expected since w' (and hence $\partial w'/\partial z$) has not as yet changed sign, hence both positive and negative vorticity are stretched and intensified. After $t' = 1.0$ the downdraft begins and intensifies, $\partial w'/\partial z'$ is negative where w' is negative and vortex *compression* occurs; the negative part of the vortex pair is greatly diminished by $t' = 2.0$.

An important feature at this low level is that the *$\zeta'_{\max}$ moves from the right side of the updraft ($t' = 0.0$, 1.0) through $w'_{\max}$ ($t' = 1.5$, not shown) then to the left side very close to the updraft/downdraft boundary* ($t' = 2.0$). The reason this occurs in this model is as follows. Vorticity is originally produced by the tilting term which is maximum where $\partial w'/\partial y'$ is maximum (positive). It is easy to see from (12) that w' maximizes at $y' = \pm\alpha t'$, so α may be identified with a nondimensional propagation velocity directed to the right (minus sign) of the mean wind. As the updraft moves to the right at a speed α, the vorticity is tilted into the vertical and subsequently stretched. Although $\partial w'/\partial y'$ becomes negative to the left of $w'_{\max}$ the prevailing vorticity is positive and continues to intensify until $\partial w'/\partial z'$ becomes negative (which, in this model, corresponds to $w' < 0$). I have repeated the calculations leading to Figs. 2a–2c (where $\alpha = 1$) with $\alpha = 0.5$ and $\alpha = 2$. The time development of w' and ζ' follows in the same fashion except for being less (more) rapid with $\alpha = 0.5$ (2).

5. Comparison with an observational case study

The preceding section demonstrates that a relatively simple model can explain (to a degree) the vorticity distribution obtained in a complex numerical simulation model. Now I would like to compare the simulation model and the present model with a particularly well-documented case study. This case (8 June 1974, near Harrah, Oklahoma) was studied by Ray (1976), Brandes (1978) and Heymsfield (1978). A comparison of the complex, but still highly idealized, numerical simulation of WK to some figures of Brandes will be given.

Fig. 5 contains the Doppler-derived vertical velocity and vorticity pattern at 1553 CST at 5.8 km (~mid-level) and 0.3 km (a low-level). The storm motion was from 230° at 13 m s^{-1} while the mean flow was from 225° at 27 m s^{-1}. Hence, the storm traveled slower than and (slightly) to the right of the mean wind. So, for comparison, identify 230° as the x direction. Hence, when I say left, I mean left facing the positive, x-direction. Now let us focus attention on the flow at 5.8 km. There are two prominent downdrafts astride the main updraft. The one on the *left* is to be compared with that of Fig. 4a ($z = 2.75$ m) and Fig. 2c (level of $\partial w/\partial z = 0$). The one on the right does not appear in the model and is discussed by Brandes. The vorticity distribution at this level may be characterized as a vortex pair with roughly equal magnitudes of the cyclonic and anticyclonic parts. The positive vorticity maximum is just to the right of the vertical velocity maximum while negative vorticity maximum is just to the right of the negative minimum of vertical velocity; these observations are in agreement with Fig. 4a. The present model (Fig. 2c) also correctly predicts the positions of the vorticity extrema vis-à-vis the vertical velocity pattern, however, it incorrectly produces a vortex pair with more negative vorticity than positive. The choice of w' in (12) dictates that $\partial w'/\partial y'$ becomes very large (negative) between the updraft and downdraft. This together with the linearization of the tilting term ($\bar{U}_z w_y$), indicates the production of large negative vorticity.

Now consider the flow at 0.3 km. Again, consider the updraft together with the downdraft on the left side as the updraft/downdraft pair discussed in the present model. The vorticity distribution is completely dominated by positive values. This agrees with Figs. 4b and 2c. Unlike the left downdraft at 5.8 km, the left downdraft at 0.3 km (at this time) extends horizontally around the rear and over to the right. This shift in the updraft/downdraft pattern is captured in Fig. 4b, but not in the present model. In our simple model, the updraft/downdraft pair moves to the right of the mean wind, the imaginary line separating updraft from downdraft is prescribed to remain parallel to the x axis as it moves rightward. As already mentioned, this tends to produce large cyclonic vorticity on the right side of the imaginary line (but to the left of the updraft maximum) and small anticyclonic vorticity on the left side of the imaginary line. Owing to this imbalance, between positive and negative vorticity, one can envision (Fig. 6) the imaginary line becoming distorted (at the mature stage) in such a way as to have the downdraft extending around the rear and over to the right as observed in Figs. 5d and 4b. The position of the vorticity maximum in the observations is between (but within) the updraft and (what I speculate to be

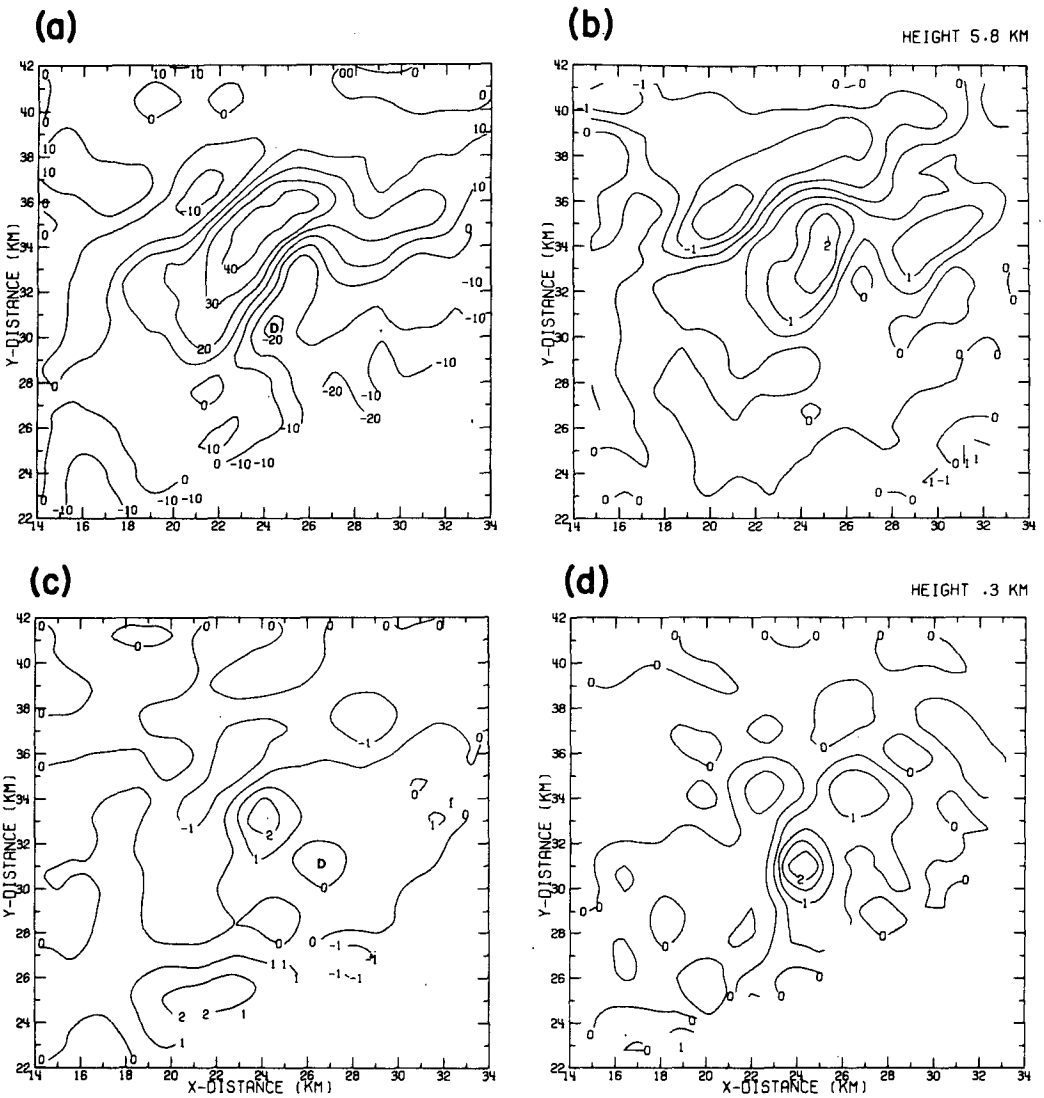

FIG. 5. Doppler-derived vertical velocity patterns at (a) 5.8 km (contour interval = 10 m s^{-1}) and (c) 0.3 km (contour interval = 1 m s^{-1}) and Doppler-derived vertical vorticity patterns at (b) 5.8 km and (d) 0.3 km (contour interval = 0.5 × 10^{-2} s^{-1}) for the Harrah storm (8 June 1974) while tornado is on the ground (1553 CST) (after Brandes, 1978).

the rearward extension of) the left-flank downdraft as occurs in the present model. The numerical model as it was circa 1978 had too coarse a grid size (horizontal resolution = 2 × 10^3 m) to detect such a fine distinction.

6. Summary

A vertical velocity field [Eq. (12)] is chosen which imitates that of the initial stages of cloud development as simulated by WK. With this an approximate version of the vertical vorticity equation (linearized about a mean westerly wind which increases with height but including the vortex stretching term) is solved. The solution agrees qualitatively (a vortex pair, vorticity extrema at proper location relative to vertical velocity extrema) with WK's numerical model solutions at z = 2.75 km which is characteristic of the mid-level flow in that model. At lower levels the positive vorticity is far greater than the negative; the indication from the numerical model and observational studies is that vortex stretching is important. The solutions demonstrate the importance of convergence at low levels to produce the roughly single-signed vortex traveling to the right of the mean wind consistent with Barnes'

model. Further support for these ideas comes from dual-Doppler radar studies. Although often overlooked, this flow structure has been observed for quite some time now. Fig. 7 is reproduced from an early paper by Stout (1957).

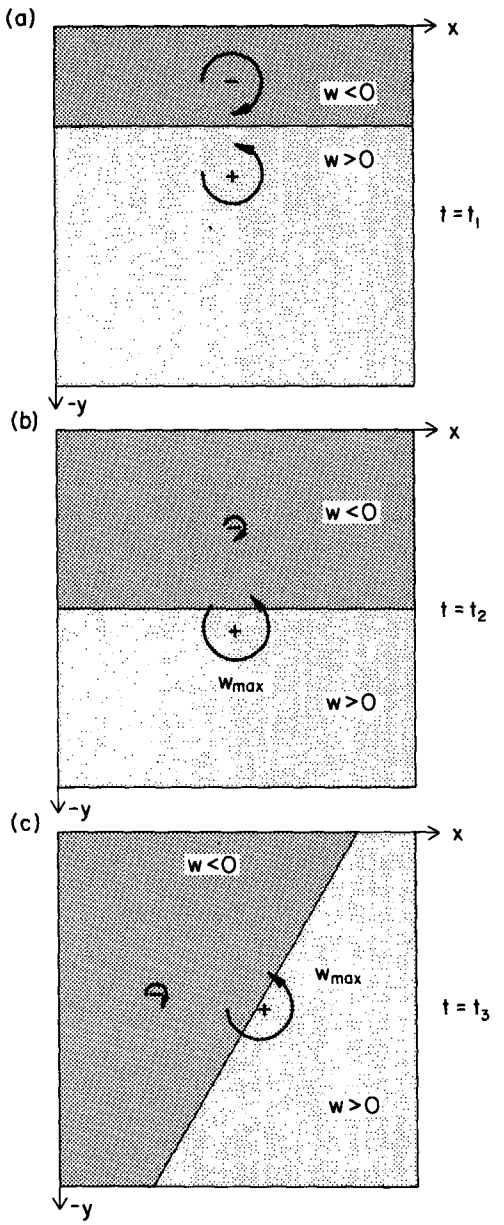

FIG. 6. Schematic of low-level vertical vorticity/vertical velocity pattern. (a) At $t = t_1$, an updraft/downdraft pair propagates toward the right (facing toward positive x). A vortex couplet is produced by tilting of mean vortex lines. (b) At a later stage, owing to convergence on the updraft side and divergence on the downdraft side, the cyclonic member is greatly enhanced. (c) At the mature stage, I speculate that the unbalanced cyclonic vorticity tends to wrap the left-flank downdraft around the rear and to the right.

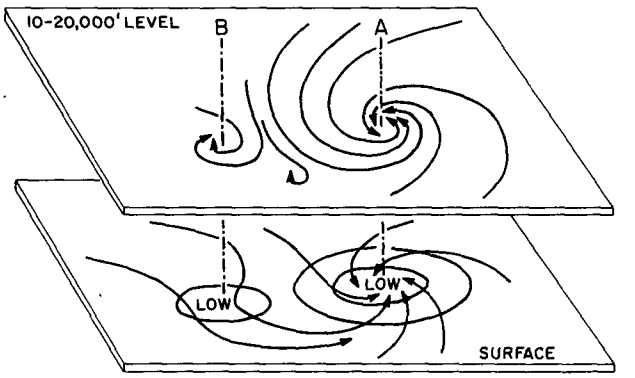

FIG. 7. Initiation of dynamically induced anticyclone vortex draft of diameter ~ 5 m in diameter (after Stout 1957).

Among the questions which remain to be answered is "Why is the right-moving cyclonic storm favored over the left-moving anticyclonic storm in nature?". Klemp and Wilhelmson (1978) show that the Coriolis force, or a clockwise curvature of wind hodograph both tend to favor the cyclonic storm. In either case the development of storm rotation is not drastically different from that discussed here, hence I believe the present results are generally relevant.

Acknowledgments. I would like to thank Drs. K. Emanuel, D. K. Lilly and an anonymous reviewer for their comments on the original manuscript.

REFERENCES

Barnes, S. L., 1970: Some aspects of a severe, right-moving thunderstorm deduced from mesonetwork rawinsonde observations. *J. Atmos. Sci.*, **27**, 634–648.

Batchelor, G. K., 1967: *An Introduction to Fluid Dynamics.* Cambridge University Press, 617 pp.

Blechman, J. R., 1980: Vortex generation in a nested grid numerical thunderstorm model. University of Wisconsin Rep. 80-1, 119 pp.

Bluestein, H. B., and C. J. Sohl, 1979: Some observations of a splitting severe thunderstorm. *Mon. Wea. Rev.*, **107**, 861–873.

Brandes, E. A., 1978: Mesocyclone evolution and tornadogenesis: Some observations. *Mon. Wea. Rev.*, **106**, 995–1011.

Clark, T. L., 1979: Numerical simulations with a three-dimensional cloud model: Lateral boundary condition experiments and multi-cellular severe storm simulations. *J. Atmos. Sci.*, **36**, 2191–2215.

Davies-Jones, R. P., 1980: Tornado dynamics. *Thunderstorm: A Social and Technological Documentary*, E. Kessler, Ed.

Dutton, J. A., 1976: *The Ceaseless Wind.* McGraw-Hill Inc., 579 pp.

Ferrel, W., 1889: *A Popular Treatise on the Winds.* Wiley, 505 pp.

Fulks, J. R., 1962: On the mechanics of the tornado. National Severe Storms Project Rep. 4, 33 pp.

Gradshteyn, I. S., and I. M. Ryzhik, 1965: *Table of Integrals, Series and Products.* Academic Press, 1086 pp.

Heymsfield, G. M., 1978: Kinematic and dynamic aspects of the

Harrah tornadic storm from dual-Doppler radar data. *Mon. Wea. Rev.*, **106**, 233–254.

Huff, F. A., H. W. Hiser and S. G. Bigler, 1954: Study of an Illinois tornado using radar. Synoptic weather and field surface data. State Water Survey Division, Urbana, IL, 73 pp.

Klemp, J. B., and R. B. Wilhelmson, 1978: Simulations of right- and left-moving storms produced through storm splitting. *J. Atmos. Sci.*, **35**, 1097–1110.

——, ——, P. S. Ray, J. Stokes, B. Johnson and K. Johnson, 1979: Comparison of modeled and observed severe storms. *Preprints 11th Conf. Severe Local Storms*, Kansas City, Amer. Meteor. Soc., 515–522.

Lilly, D. K., 1979: The dynamical structure and evolution of thunderstorms and squall lines. *Annual Review of Earth and Planetary Science*, Vol. 7, Annual Reviews, Inc., 117–161.

Ogura, Y., and N. A. Phillips, 1962: Scale analysis of deep and shallow convection in the atmosphere. *J. Atmos. Sci.*, **19**, 173–179.

Ray, P. S., 1976: Vorticity and divergence within tornadic storms from dual Doppler observations. *J. Appl. Meteor.*, **15**, 879–890.

Schlesinger, R. E., 1975: A three-dimensional numerical model of an isolated deep convective cloud: Preliminary results. *J. Atmos. Sci.*, **32**, 934–964.

——, 1978: A three-dimensional numerical model of an isolated thunderstorm: Part I Comparative experiments for variable ambient wind shear. *J. Atmos. Sci.*, **35**, 690–713.

Stout, G. E., 1957: Mesometeorological systems from dense network stations. Paper presented at IUGG Meeting, Toronto.

Wilhelmson, R. B., and J. B. Klemp, 1978: A numerical study of storm splitting that leads to long-lived storms. *J. Atmos. Sci.*, **35**, 1974–1986.